

Synthesis of a Library of Iridium-Containing Dinuclear Complexes with Bridging PNNN and PNNP Ligands (BL), [LM(μ -BL)M'L']BF₄.

2. Preparation, Basic Coordination Properties, and Reactivity of the Carbonyl Complexes

Christian Dubs, Toshiki Yamamoto, Akiko Inagaki, and Munetaka Akita*

Chemical Resources Laboratory, Tokyo Institute of Technology, R1-27, 4259 Nagatsuta, Midori-ku, Yokohama 226-8503, Japan

Received October 18, 2005

A series of dinuclear carbonyl complexes with PNNP and PNNN ligands, [(L)M(PNNX)M'(L)]BF₄ (X = P, N; M(L), M'(L') = Ir(CO)₂, Rh(CO)₂, Pd(allyl)), have been prepared by carbonylation (1 atm) of the corresponding cod complexes, and the Rh/Ir complexes have been further converted to μ - η^1 : η^2 -acetylide complexes, where effective π -back-donation to the acetylide ligand is essential to stabilize them. On the basis of the stability of the acetylide complexes, the π -donating ability of the metal fragment in the PNNX system is estimated to be (P,N)Rh > (P,N)Ir > (N,N)M. The dinuclear PNNX complexes catalyze alkyne hydrogenation, alkene hydroformylation, and allylation of aniline with allyl alcohol, and, for the allylation, a dinuclear mechanism involving activation of allyl alcohol by interaction with a CO ligand is proposed.

Introduction

In the preceding paper a unique systematic synthetic method for a series of homo- and heterodinuclear complexes with the PNNN and PNNP ligands has been reported.¹ For further extension of the library, the obtained labile cod complexes (cod = 1,5-cyclooctadiene) are converted into carbonyl and acetylide complexes, and their basic coordination properties resulting from a combination of (1) the central metals, (2) ligands, and (3) coordination sites (P,N vs N,N) have been studied.

Results and Discussion

Carbonylation of η^4 -Cyclooctadiene Complexes. The cod complexes **1'**–**5'** reported in the preceding paper are subjected to carbonylation (1 atm) (Scheme 1). The homodinuclear complex (**2'a**) and the Pd-containing complexes (**3'** and **5'**) are readily converted to the desired carbonyl complexes in a manner similar to the synthesis of **1a,b** reported by Bosnich,² but incomplete conversion and/or metal exchange are observed for the other cases, unless the carbonylation is carried out under controlled conditions. The incomplete conversion, however, can be overcome by isolation of a partly carbonylated reaction mixture followed by repeated carbonylation. In this case, the cod ligand is not completely liberated from the metal coordination sphere. For example, in carbonylation of a related P,N-coordinated mononuclear species, [(κ^2 -py-CH₂PPh₂)Ir(cod)]BF₄, a η^2 -cod-coordinated product, [(μ - η^2 : η^2 -cod){Ir(κ^2 -py-CH₂-PPh₂)(CO)₂}₂](BF₄)₂ (**6**),³ has been isolated and characterized by X-ray crystallography. Removal of the liberated cod molecule in the reaction mixture, therefore, is essential for

complete conversion to the desired carbonyl complexes. Carbonylation of the heterodinuclear complexes **1'c**, **2'b–d**, and **4'** at ambient temperature, on the other hand, produces a statistical mixture of homo- and heterometallic complexes through a metal exchange process. For example, carbonylation of **1'c** affords a 1:2:1 mixture of **1a**, **1c**, and **1b**, and that of **2'c** gives a 1:1:1:1 mixture of the four possible products, which is also obtained from the isomeric counterpart **2'd**. This metal exchange process, however, can be suppressed by conducting the carbonylation at 0 °C. The Ir(PNNN)Rh complex **2'c** is converted to **2c** by the repeated carbonylation at 0 °C, and thus, to get reproducible results, the repeated carbonylation at 0 °C is preferable for every case.

The obtained carbonyl complexes are readily characterized by the appearance of ν (CO) vibrations. The specific formation of the distinctive isomeric species **2c,d** from **2'c,d**, respectively, leads to the conclusion that the carbonylation proceeds with retention of the metal-coordinated sites, when the reaction is carried out under controlled conditions. Molecular structures of the homonuclear Rh–PNNN complex **2a** and the heteronuclear Pd(PNNN)Ir complex **5** have been determined by X-ray crystallography. Their ORTEP views and selected structural parameters are shown in Figure 1 and Table 1, respectively, and the structural features will be discussed later, together with those of related compounds. It is also found that **2a** forms cocrystals with the P-oxidized species **7** (Chart 1), which results from adventitious oxidation during a prolonged recrystallization period. Because an isolated sample of **2a** is converted into **7** upon stirring its solution in air, it is suggested that the P,N-chelate in **2a** is opened via P–Rh dissociation and the resultant free P moiety is oxidized and re-coordinated to the Ir center to furnish **7**.

Careful analysis of the carbonylation of the pair of Ir–Rh/PNNN complexes **2'c,d** reveals that the carbonylation proceeds in a stepwise manner (Scheme 2). As described in the preceding paper,¹ the deshielded H₆ signal ($\delta_{\text{H}} \sim 8$; doublet) of the pyridyl group serves as a diagnostic for the coordination of the M(cod) fragments (M = Ir, Rh) to the N,N site.¹ On going from **2'c** to

(1) Dubs, C.; Yamamoto, T.; Inagaki, A.; Akita, M. *Organometallics* 2006, 25, 1344.

(2) (a) Schenk, T. G.; Downs, J. M.; Milne, C. R. C.; Mackenzie, P. B.; Boucher, H.; Whelan, J.; Bosnich, B. *Inorg. Chem.* 1985, 24, 2334. (b) Schenk, T. G.; Milne, C. R. C.; Sawyer, J. F.; Bosnich, B. *Inorg. Chem.* 1985, 24, 2338. (c) Bosnich, B. *Inorg. Chem.* 1999, 38, 2554.

(3) Complex **6** is obtained as a minor byproduct of the carbonylation and has been characterized only by X-ray crystallography. Crystallographic data are included in the Supporting Information.

Scheme 1

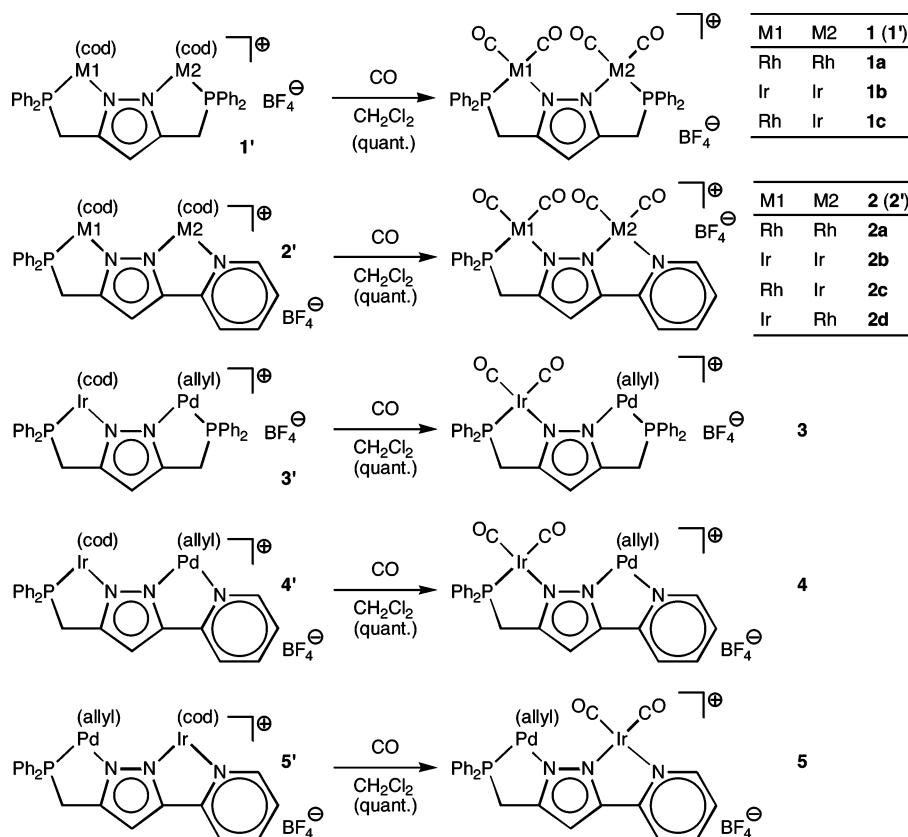
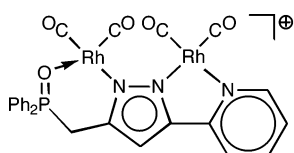
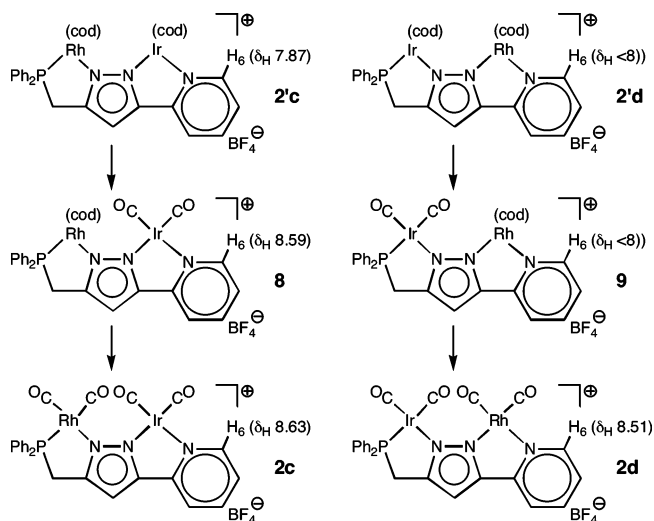


Chart 1



Scheme 2



the half-carbonylated species **8** (Scheme 2) and then to **2c**, the $\delta_{\text{H}}(\text{H}_6\text{-py})$ signals are shifted from 7.87 ppm (**2'c**: (N,N)Ir(cod)) to 8.59 ppm (**8**: (N,N)Ir(CO)₂) and then to 8.63 ppm (**2c**: (N,N)Ir(CO)₂). Therefore, it is concluded that the (N,N)Ir(cod) part is carbonylated at the stage of **8**. On the other hand, carbonylation of **2'd** causes shifts of the H₆ signals as follows: <8 ppm (**2'd**: overlapped with the other signals; (N,N)Rh(cod))

→ <8 ppm (**9**: overlapped with the other signals; (N,N)Rh(cod)) → 8.51 ppm (**2d**: (N,N)Rh(CO)₂). In this case, therefore, the (N,N)Rh(cod) part is carbonylated at the final stage. The stepwise conversions can also be followed by IR, but no useful information is obtained from the ³¹P NMR data, because no significant shift of the ³¹P NMR signals is observed. It is notable that the Ir(cod) parts are the preferential carbonylation sites irrespective of the coordination environment (P,N vs N,N).

μ - η^1 : η^2 -Acetylide Complexes: σ - vs π -Coordination Dependent on the Metal and Ligand Donor Sets (P,N vs N,N).^{4,5} The P,N and N,N coordination sites in the heterodinuclear complexes, in particular, in the unsymmetrical PNNN complexes, show variable coordination properties dependent upon the combination of the metals (Ir vs Rh) and the coordination sites (P,N vs N,N). The μ -acetylide complex is a convenient probe for judging the coordination properties of the coordination sites by taking a look at the σ - and π -coordination.⁶

μ -Acetylide complexes with the PNNP ligand (**10**) are prepared by treatment of the tetracarbonyl complexes of Ir and Rh (**1** and **2**) with lithium acetylide (Scheme 3) in a manner similar to the previously reported preparation of the (PNNP)-Rh₂ complexes **10aa** and **10ab**.⁵ In contrast, for the PNNN complexes, not all combinations afford the desired μ -acetylide complexes as stable species, and the preparation is successful only in the cases of complexes **11aa**, **11ab**, and **11ca** with the

(4) The obtained carbonyl PNNP and PNNN complexes were subjected to the reactions examined for **1a** (e.g. alkyne, hydrosilane),⁵ but intractable mixtures of products were obtained, suggesting considerably different reactivity between the Rh and Ir analogues.

(5) (a) Tanaka, S.; Inagaki, A.; Akita, M. *Angew. Chem., Int. Ed.* **2001**, *40*, 2865. (b) Tanaka, S.; Dubs, C.; Inagaki, A.; Akita, M. *Organometallics* **2004**, *23*, 317. (c) Tanaka, S.; Dubs, C.; Inagaki, A.; Akita, M. *Organometallics* **2005**, *24*, 163. (d) Dubs, C.; Inagaki, A.; Akita, M. *Chem. Commun.* **2004**, 2760.

(6) Lotz, S.; van Rooyen, P. H.; Meyer, R. *Adv. Organomet. Chem.* **1995**, *37*, 219.

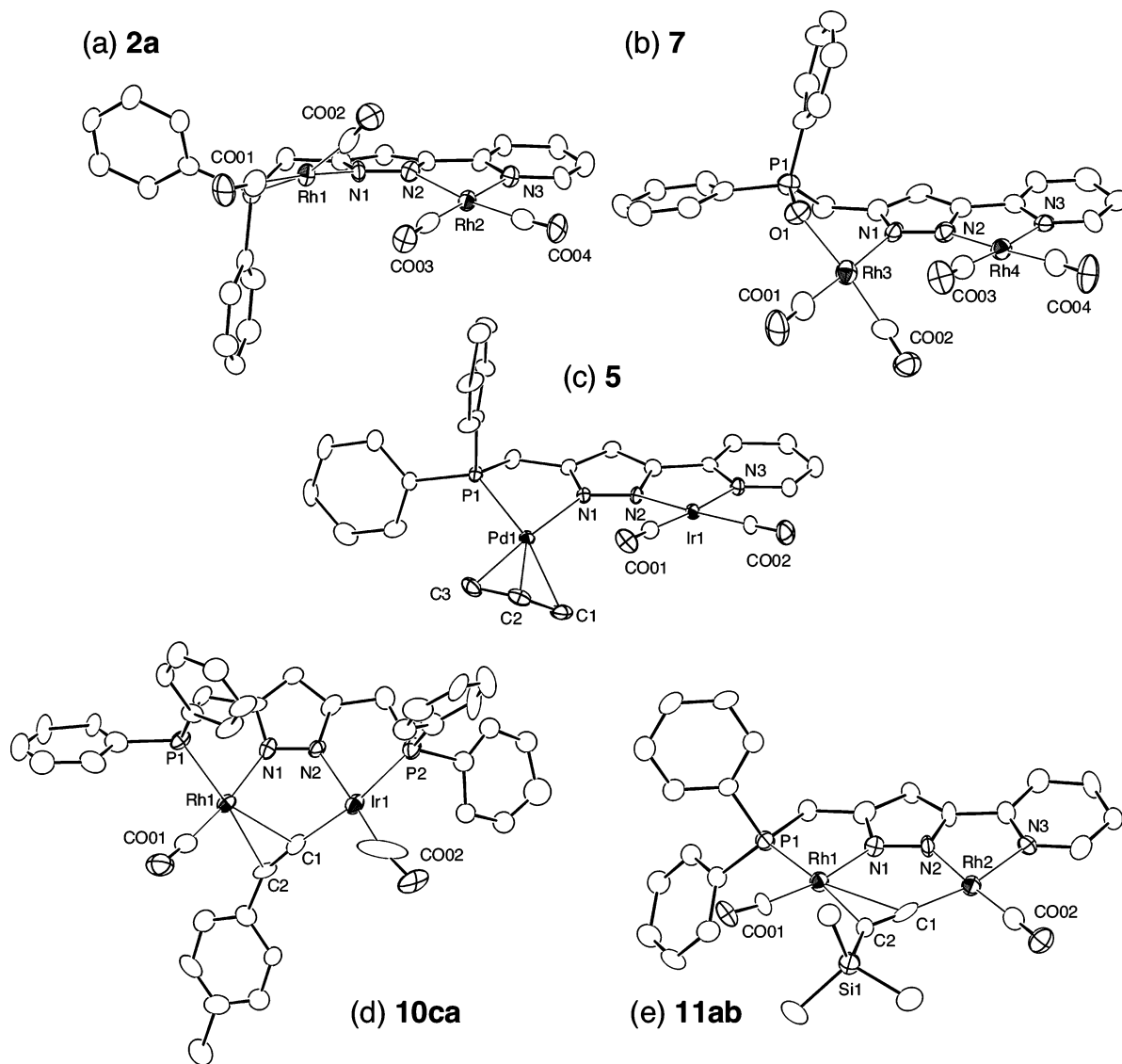


Figure 1. Molecular structures of (a) **2a**, (b) **7**, (c) **5**, (d) **10ca**, and (e) **11ab** drawn with thermal ellipsoids at the 30% probability level.

particular Rh(PNNN)M metal arrangement. While the μ -acetylide complexes appear to be formed for the other cases (**11ba** and **11da**), they decompose during the isolation process. In addition, the isolated complexes **11aa** and **11ca** turn out to be much less stable than the PNNP complexes **10**.

The obtained μ -acetylide complexes have been characterized by spectroscopic and crystallographic analyses. The homonuclear Ir₂(PNNP) complexes **10b** show dynamic behavior via a windshield wiper like motion, as usually observed for symmetrical μ -acetylide complexes, including the previously reported Rh₂ analogues **10a**.^{5c} When the temperature is lowered, the symmetrical NMR features change into ones consistent with an unsymmetrical structure, suggesting that the dynamic behavior is frozen out at low temperatures. For example, the single ³¹P signals for the C≡CSiMe₃ complexes separate into two signals below 0 °C (**10bb**; Ir) and -40 °C (**10ab**; Rh). When the separations of the two signals at a slow exchange limit are taken into account (1296 Hz (**10ab**; Rh) ≫ 245 Hz (**10bb**; Ir)), it is concluded that the activation barrier for the Ir complex is much higher than that for the Rh complex. The activation energies at the coalescence temperatures are estimated to be 9.8 kcal mol⁻¹ (**10ab**; Rh) and 12.5 kcal mol⁻¹ (**10bb**; Ir).⁷

In contrast, the heteronuclear complexes **10c** are static with respect to the windshield wiper motion, but the coordination

sites cannot be determined by the spectroscopic data alone. X-ray crystallography reveals that the *p*-tol-C≡C complex **10ca** (Figure 1 and Table 1) has the acetylide ligand σ -bonded to Ir and π -bonded to Rh. The same coordination feature is also found for the Me₃SiC≡C complex **10bb**, although the quality of the crystal is low.⁸ Comparison of the structures and the ³¹P NMR data for the previously reported Rh₂ complexes **10a** reveals that, of the two ³¹P signals for **10ab** (observed at -80 °C), the signal with the larger $J_{\text{Rh-P}}$ coupling constant appearing at lower field (δ_{P} 55.3 (d, $J_{\text{Rh-P}}$ = 159 Hz)) can be assigned to the phosphorus atom coordinated to the π -bonded Rh center and the other signal with the smaller $J_{\text{Rh-P}}$ coupling constant appearing at higher field (δ_{P} 47.3 (d, $J_{\text{Rh-P}}$ = 122 Hz)) can be assigned to the phosphorus atom coordinated to the σ -bonded Rh center (Chart 2). This assignment turns out to be useful in the characterization of **11ca**, as described below.

As for the ¹³C NMR data, it is difficult to locate the signals for the C≡C part because of their low intensities, owing to

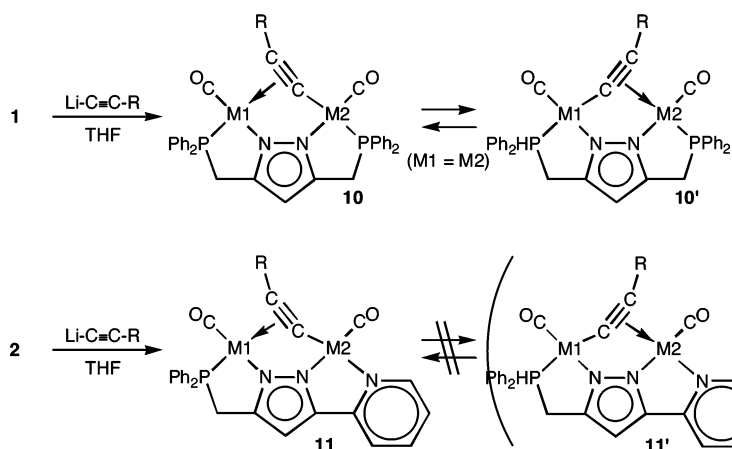
(7) Bovey, F. A.; Jelinski, L.; Mirau, P. A. *Nuclear Magnetic Resonance Spectroscopy*, 2nd ed.; Academic: San Diego, CA, 1988.

(8) Because of the low quality of the crystal, the result for **10bb** is not included in this paper. Crystal data for **10bb**: triclinic, space group *P1*, *a* = 17.553(6) Å, *b* = 19.473(7) Å, *c* = 11.441(4) Å, α = 98.91(3)°, β = 90.17(2)°, γ = 65.268(9)°, *V* = 3500(2) Å³, *Z* = 4, *T* = -60 °C.

Table 1. Selected Structural Parameters for the Carbonyl and μ -Acetylide Complexes^a

	2a^b	5	7	10ca	11ab
ML	Rh(CO) ₂	Pd(allyl)	Rh(CO) ₂	Rh(CO)	Rh(CO)
M'L'	Rh(CO) ₂	Ir(CO) ₂	Rh(CO) ₂	Ir(CO)(C≡C- <i>p</i> -tol)	Rh(CO)(C≡CSiMe ₃)
X	py	py	py/P=O	CH ₂ PPh ₂	py
M...M'	4.253(1)	4.336(1)	4.166(2)	3.656(1)	3.877(2)
M-P1	2.312(3)	2.281(2)	2.063(8) ^b	2.284(5)	2.236(4)
M-N1	2.084(8)	2.111(6)	2.100(9)	2.03(1)	2.08(1)
M'-N2	2.071(7)	2.042(6)	2.058(9)	2.258(4)	1.94(1)
M'-X	2.100(8)	2.103(7)	2.12(1)	2.08(1)	2.13(1)
M-L	1.86(1) (C01A) 1.92(1) (C02A)	2.23(1) (C1) 2.14(1) (C2) 2.08(1) (C3)	1.86(1) (C01B) 1.83(1) (C02B)	2.05(2) (C1) 1.62(3) (C02)	2.56(1) (C1) 2.31(1) (C2) 1.83(1) (C01)
M'-L'	1.84(1) (C03A) 1.86(1) (C04A)	1.859(9) (C01) 1.871(9) (C02)	1.85(1) (C03B) 1.86(1) (C04B)	2.32(1) (C1) 2.29(1) (C2) 1.81(2) (C01)	2.01(2) (C1) 1.79(2) (C02)
∠P1-M-N1	80.1(2)	80.5(2)	88.0(3)	80.1(3)	80.4(3)
∠N2-M'-X	78.4(3)	77.9(3)	79.7(3)	77.2(3)	77.2(5)
∠M-N1-N2-C13	171.2(6)	167.2(5)	169.9(7)	167(1)	173.6(9)
∠M'-N2-N1-C11	159.8(7)	162.7(6)	171.8(8)	169(1)	177(1)
∠M-N1-N2-M'	29(1)	29(1)	21(1)	0(2)	12(2)

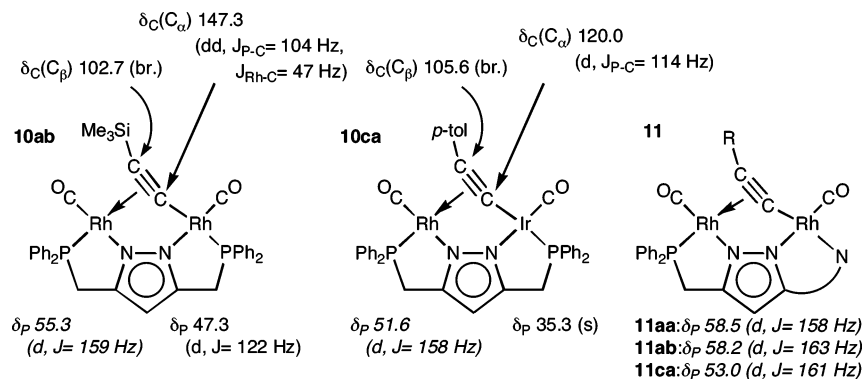
^a Interatomic distances in Å and bond angles and dihedral angles in deg. ^b **2a** and **7** formed cocrystals.

Scheme 3

M1	M2	R	10
Rh	Rh	<i>p</i> -Tol	10aa (71 %) ^a
Rh	Rh	SiMe ₃	10ab (76 %) ^a
Ir	Ir	<i>p</i> -Tol	10ba (33 %)
Ir	Ir	SiMe ₃	10bb (53 %)
Rh	Ir	<i>p</i> -Tol	10ca (85 %)
Rh	Ir	SiMe ₃	10cb (65 %)

^a: taken from ref. 5c.

M1	M2	R	11
Rh	Rh	<i>p</i> -Tol	11aa (63 %)
Rh	Rh	SiMe ₃	11ab (46 %)
Ir	Ir	<i>p</i> -Tol	11ba (0 %)
Rh	Ir	<i>p</i> -Tol	11ca (35 %)
Ir	Rh	<i>p</i> -Tol	11da (0 %)

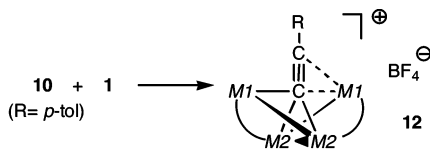
Chart 2

complicated coupling with the P and Rh nuclei. However, the data for the Rh(PNNP)Ir(C≡C-*p*-tol) complex **10ca** are comparable to those for the previously reported symmetrical Rh₂ complex **10ab**, as shown in Chart 2. The couplings of the magnitude of ~110 Hz can be attributed to J_{C-P} couplings with the phosphorus atom attached to the σ -bonded Rh center, because the coupling of $J = 47$ Hz disappears upon replacement

of the σ -bonded metal (Rh: **10ab** → Ir: **10ca**). The coupling of $J = 47$ Hz for **10ab** is, therefore, attributed to the J_{Rh-C} coupling with the σ -bonded Rh center.

The coordination mode of the unstable Rh(PNNN)M complex **11** can be determined by comparison of the ³¹P NMR data. As discussed above (Chart 2), the ³¹P data (δ_P and J_{C-P}) for **11** are comparable to those for one of the two types of ³¹P NMR signals

Scheme 4



entry	10	1	results
1	10aa (Rh ₂)	1a (Rh ₂)	12a (56 %)
2	10ba (Ir ₂)	1b (Ir ₂)	unident. products (u.p.)
3	10ca (Rh-Ir)	1c (Rh-Ir)	12b (93 %; M ₁ = Rh, M ₂ = Ir)
4	10aa (Rh ₂)	1b (Ir ₂)	12a + u.p.
5	10ba (Ir ₂)	1a (Rh ₂)	12a + u.p.
6	10ca (Rh-Ir)	1a (Rh ₂)	12a + 12b + u.p.
7	10ca (Rh-Ir)	1b (Ir ₂)	12b + u.p.

for the PNNP complex **10**, i.e., the deshielded signal with a larger Rh–P coupling constant, indicating that the acetylide ligand in **11** is π -bonded to the Rh(P,N) part and, as a consequence, σ -bonded to the M(N,N) center. The molecular structure of the rather stable homonuclear dirhodium complex **11ab** is determined by X-ray crystallography (Figure 1(e)), and the π -coordination of the (P,N)Rh part rather than the (N,N)Rh part has been confirmed.

On consideration of the successfully isolated μ -acetylide complexes, it is noteworthy that, for the series of the PNNP and PNNN complexes, the μ -acetylide complexes are stable enough to be isolated only when a Rh(P,N) fragment is π -coordinated to the bridging acetylide ligand. While the Ir(PNNP)Ir complexes **10b** are isolable, they are less stable than the Rh analogues **10a** and, therefore, the yields are modest. Two ways of back-donation are feasible toward a μ -acetylide ligand: (1) to the antibonding π^* -orbitals of the C \equiv C part, leading to an η^2 -coordinated structure, and (2) to the vacant p-orbital of the α -carbon atom, leading to partial double bond M=C $_{\alpha}$ character. However, in general, the latter interaction is not as significant as that of other good π -acceptors such as CO.⁹ On the other hand, the P,N-donor set is a better π -donor compared with the N,N-donor set but, as for the metal center, the general tendency of the electronic properties of second- and third-row metals is not straightforward and still controversial.¹⁰ Judging from the results obtained, the π -interaction (1) appears to contribute to stabilization of the μ -acetylide complex and, therefore, the Rh center is more π -donating than the Ir center; thus, the π -donating ability is estimated to be in the order of Rh(P,N) > Ir(P,N) > M(N,N).

In a previous paper we reported unique tetrarhodium μ_4 -acetylide complexes with the PNNP ligand **12**, which were prepared by reaction between **10a** and **1a**.⁵ The newly prepared dinuclear μ -acetylide complexes with the PNNP ligand **10** are subjected to reaction with **1** (Scheme 4). In this case, too, the stability of the adducts is dependent on the metal.¹¹ In reactions of **10** and **1** of the same M₁–M₂ combination (entries 1–3), the adducts **12a** and **12b** are formed, only when Rh is included in both components (entries 1 and 3), and a mixture of unidentified products is obtained from **10ba** and **1b** (entry 2). For entries 4–7 of different metal combinations, mixtures containing **12a** and/or **12b** and unidentified products are formed,

as determined by ESI-MS and ³¹P NMR analyses. The heterotetranuclear complex **12b** has been characterized by spectroscopic data, and the arrangement of the metals (M₁ = Rh, M₂ = Ir) is tentatively assigned according to the tendency observed for the dinuclear μ -acetylides: Rh prefers the π -coordinating site. The formation of the mixtures (entries 2 and 4–7) should involve dissociation into dinuclear species, where acetylide transfer to the Rh-containing dinuclear fragment leads to the formation of **12a** and **12b**, and the other components should decompose to give the unidentified products.

Catalytic Reactions. Polynuclear complexes are expected to show unique features, which are not observed for mononuclear complexes, by sharing the functions needed for catalytic processes. The obtained dinuclear complexes have been subjected to a couple of typical catalytic reactions.

(i) Hydrogenation and Hydroformylation. Catalytic hydrogenation of alkenes and alkynes with [(PNNP)Rh₂(nbd)₂]-BF₄ and **1b** was reported by Bosnich, but features peculiar to the dinuclear systems were not observed.² All cod complexes **1'** and **2'** show activity for catalytic hydrogenation of diphenylacetylene, and a mixture of *cis*- and *trans*-stilbene and 1,2-diphenylethane is obtained, when the reaction is carried out in the presence of the catalyst (1 mol %) under an H₂ atmosphere (5 atm) in THF (2 mL; MeOH (0.2 mL) was added to **2'a** and **2'b** to dissolve them). The order of catalytic activities is as follows (the numbers given in parentheses are conversion of diphenylacetylene/yield of *cis*-stilbene/yield of *trans*-stilbene/yield of diphenylethane, in percent): for the PNNP series, **1'b** (100/0/60/39) \approx **1'c** (100/0/60/31) > **1'a** (33/27/5/0); for the PNNN series, **2'b** (100/0/53/46) \approx **2'd** (100/0/51/48) > **2'c** (47/40/7/0) > **2'a** (8/4/0/0). The hydrogenation proceeds in a stepwise manner, as confirmed by comparison with hydrogenation of stilbenes (PhC \equiv CPh \rightarrow *cis*-PhCH=CHPh \rightarrow *trans*-PhCH=CHPh \rightarrow PhCH₂CH₂Ph), and no significant feature peculiar to the dinuclear systems has been observed, in accord with the report by Bosnich.

The cod complexes **1'** and **2'** are also effective for hydroformylation of 1-octene to give a mixture of nonanal and 2-methyloctanal, with the former being the major product (*n/i* \approx 2) when the reaction is conducted for 6 h at 80 °C under a CO (15 atm)–H₂ (15 atm) mixture. The activity determined on the basis of the conversion of 1-octene is as follows (the numbers given in parentheses are conversion of 1-octene/yield of nonanal/yield of 2-methyloctanal, in percent): **1'a** (80/41/25) \approx **2'c** (77/42/21) > **2'd** (66/44/21) \approx **1'b** (61/29/11) > **1'c** (37/22/11). The Rh-containing complexes appear to be more active than the Ir-containing ones, but metal exchange reaction occurs during the catalytic reaction of the heterometallic complexes, as revealed by ESI-MS analysis of the reaction mixtures,¹² being in accord with the metal exchange observed for the carbonylation of the cod complexes described above.

(ii) Catalytic Allylation of Aniline with Allyl Alcohol. Catalytic allylic substitution has been mediated by a variety of transition-metal species.¹³ Although allyl halide and esters have been used as allylic sources, very few successful direct catalytic allylations with allyl alcohol have been reported so far, despite its advantage from the viewpoint of economical and environ-

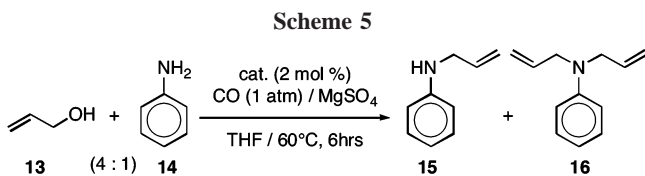
(9) (a) Lichtenberger, D. L.; Renshaw, S. K.; Wong, A.; Tagge, C. D. *Organometallics* **1993**, *12*, 3522. See also: (b) Lichtenberger, D. L.; Renshaw, S. K.; Bullock, R. M. *J. Am. Chem. Soc.* **1993**, *115*, 3276.

(10) Mingos, D. M. P. *Essential Trends in Inorganic Chemistry*; Oxford University Press: Cambridge, U.K., 1998.

(11) From the reactions of the PNNN complexes **11** no characterizable product could be obtained.

(12) The cod complexes were converted to the corresponding CO complexes during the hydroformylation.

(13) See for example: Tsuji, J. *Transition Metal Reagents and Catalysts: Innovations in Organic Synthesis*; Wiley: New York, 2002. Tsuji, J. *Palladium Reagents and Catalysts: New Perspectives for the 21st Century*; Wiley: New York, 2004.



entry	cat.	conv. of 14	yield of 15	yield of 16
1	3 [Ir(PNNP)Pd]	93	58	35
2	4 [Ir(PNNN)Pd]	72	35	0
3	5 [Pd(PNNN)Ir]	40	38	2
4	1b [Ir(PNNP)Ir]	20	20	0
5	17 [Pd(PNNP)Pd] ^a	98	57	37

^a **17**: [(η^3 -allyl)Pd(PNNP)Pd(η^3 -allyl)]BF₄.

mental concerns.¹⁴ Then the (η^3 -allyl)Pd–Ir complexes have been employed as catalysts for allylation of aniline (**14**). As a result, all complexes show catalytic activity to give a mixture of mono- (**15**) and diallylaniline (**16**), when the reaction is carried out for 6 h at 80 °C in the presence of MgSO₄ under a CO atmosphere (1 atm) (Scheme 5). CO appears to suppress decomposition of the catalytic species and, in entries 2 and 5, formation of byproducts, which cannot be detected by GLC, is evident. It is notable that the diiridium complex **1b** shows catalytic activity, though the activity is inferior to that of the Pd-containing complexes. However, no apparent relationship between the activity and the coordination sites is observed.

To obtain information of the reaction mechanism at an early stage, a stoichiometric reaction of the Ir(PNNP)Pd complex **3** with allyl alcohol **13** has been examined (Figure 2). Addition of 1 equiv of **13** to **3** causes broadening of the ³¹P NMR signals, and in particular, the signal for the Ir(PN) part becomes undetectable (Figure 2b). However, upon further addition of 10 equiv of **13** a broad signal appears around 9 ppm (Figure 2c), and final treatment with NEt₃ gives four pairs of sharp signals (Figure 2d), which are identical with the spectrum of the product **19** isolated from the mixture. When the reaction is followed by IR, no apparent change is observed before addition of NEt₃, which causes appearance of a new set of two absorptions. The four sets of the ³¹P NMR signals observed for **19** reveal that it consists of four stereoisomers, which show the same IR features within the experimental IR resolution, and is tentatively assigned to the (allyloxy)carbonyl species on the basis of the IR spectrum containing a terminal CO vibration (1962 cm⁻¹) and an acyl C=O vibration (1654 cm⁻¹), although NMR characterization is hampered by the presence of the four isomers. The spectral changes mentioned above can be interpreted in terms of Scheme 6. Complexes **3** and **13** are in equilibrium with the adduct **18**, and the equilibrium is shifted to the reactant side (**3** + **13**), but addition of a large amount of **13** causes an increase of population of **18** enough for it to appear as a broad signal. The acidic OH proton in **18** is removed upon addition of NEt₃, and the neutral species **19** is obtained.

The structure of **18** suggests three possible mechanisms for the subsequent allylation processes: i.e., (1) a Pd-centered

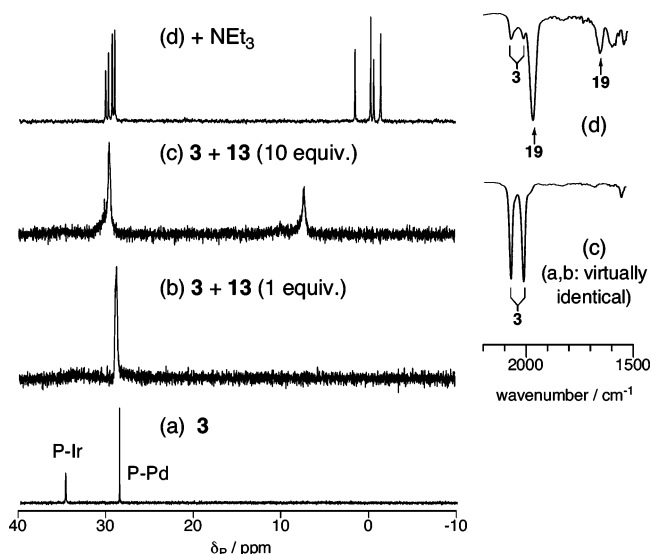


Figure 2. Interaction of **3** with allyl alcohol (**13**) followed by ³¹P NMR and IR: (a) **3**; (b) after addition of 1 equiv of **13**; (c) after addition of 10 equiv of **13**; (d) after addition of NEt₃.

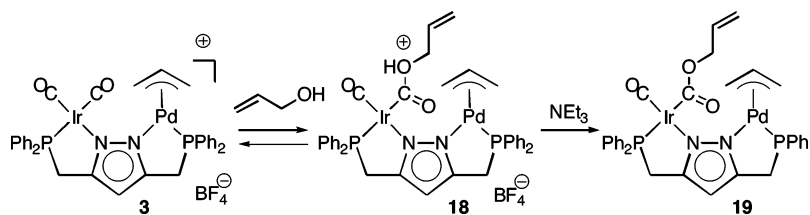
mononuclear mechanism, (2) an Ir-centered mechanism involving conversion of the (allyloxy)carbonyl–Ir part into a (η^3 -allyl)–Ir species, and (3) a dinuclear mechanism, which follows (i) activation of allyl alcohol via the (allyloxy)carbonyl–Ir species, (ii) subsequent transfer of the allyl moiety to the Pd center accompanying C–O bond cleavage, and (iii) reaction at the resultant (η^3 -allyl)Pd moiety. Although it is difficult to determine the mechanism of the present complicated dinuclear system, the present result suggests that formation of a (η^3 -allyl)metal species from allyl alcohol may be promoted by the initial interaction with the CO ligand (as in **18**). C–O bond cleavage of alcohol is not always a facile process, and dehydration under acidic conditions is most frequently referred to as the C–O bond activation method,¹⁴ while the ultimate driving force of the present system is still acid-catalyzed dehydration. The mechanistic study is now under way, with related mononuclear complexes having the partial structures (with P,N and N,N chelates) of the dinuclear complexes, and the results will be reported in a forthcoming paper.

Molecular Structures of Carbonyl and Acetylide Complexes. The carbonyl complexes **2a** and **5** and the μ -acetylide complexes **10ca** and **11ab** have been characterized by X-ray crystallography together with complex **7** resulting from the adventitious P-oxidation (Figure 1 and Table 1).

The absence of metal–metal interaction is evident from the intermetallic distances (>3.6 Å). All metal centers adopt square-planar coordination geometries, as usually observed for four-coordinate d⁸-metal complexes with 16 valence electrons, and coordination of the allyl ligand in **5** is unsymmetrical, owing to the trans effect of the phosphorus atom. Distortion of the core structures from planar ones is also noted for the carbonyl complexes **2a**, **7**, and **5**, as observed for the precursors **1'** and **2'**. The distortion can be best described by the $\angle M-N1-N2-M'$ dihedral angle, and the extent of the distortion is considerably smaller than that of the cod complexes **1'** and **2'** because of the linear structure of the CO ligands. The comparable torsion angles for **2a** with the five-membered Rh,P-containing metallacycle and **7** with the six-membered Rh,O,P-containing metallacycle reveal that the distortion mainly results from the steric repulsion between the inner ligands not from the strain of the Rh,P,(O)-containing metallacycle. In contrast, the core structures of the μ -acetylide complexes are

(14) (a) Ozawa, F.; Okamoto, H.; Kawagishi, S.; Yamamoto, S.; Minami, T.; Yoshifuji, M. *J. Am. Chem. Soc.* **2002**, *124*, 10968. (b) Ozawa, F.; Ishiyama, T.; Yamamoto, S.; Kawagishi, S.; Murakami, H.; Yoshifuji, M. *Organometallics* **2004**, *23*, 1698. (c) Bricout, H.; Carpentier, J.-F.; Mortreux, A. *J. Mol. Catal. A* **1998**, *136*, 242. (d) Sakaibara, M.; Ogawa, A. *Tetrahedron Lett.* **1994**, *35*, 8015. (e) Yang, S.-C.; Tsai, Y.-C. *Organometallics* **2001**, *20*, 763. (f) Tamaru, Y. *J. Organomet. Chem.* **1999**, *576*, 215. (g) Kimura, M.; Futama, M.; Shibata, K.; Tamaru, Y. *Chem. Commun.* **2003**, 234. (h) García-Yebra, C.; Janssen, J. P.; Rominger, F.; Helmchen, G. *Organometallics* **2004**, *23*, 5459.

Scheme 6



virtually planar, because the μ -acetylide ligand occupies the inner two coordination sites in a μ - η^1 : η^2 fashion. The rather larger M...M separations make the π -coordinating M1-C α interaction longer than those in M-M-bonded systems. The M1-C α -C β triangle in **11ab** is much more distorted from an isosceles triangle than that in **10ca**, as can be seen from ($d(\text{M}-\text{C}_\alpha) - d(\text{M}-\text{C}_\beta) = 0.25 \text{ \AA} (\mathbf{11ab}) > 0.03 \text{ \AA} (\mathbf{10ca})$), presumably owing to the larger M...M separation for **11ab**.

Conclusion. The Ir-containing dinuclear cod complexes with the PNNP and PNNN complexes have been successfully converted to the corresponding carbonyl complexes by treatment with CO (1 atm). The obtained carbonyl complexes have been further converted to the μ -acetylide complexes to examine the basic coordination properties of the ancillary PNNP and PNNN ligand, and the properties of the P,N and N,N chelates on dinuclear complexes have been established. Combined with the results of the preceding paper,¹ a library of Ir-containing homo- and heterodinuclear complexes have been established, as summarized in Chart 3.

The obtained dinuclear complexes serve as catalysts for alkyne hydrogenation, alkene hydroformylation, and allylation with allylic alcohol, and a dinuclear mechanism has been proposed for the allylation, the mechanism of which needs to be confirmed by further study and will be the subject of a forthcoming paper.

Experimental Section

General Methods. All manipulations were carried out under an inert atmosphere by using standard Schlenk tube techniques. Solvent purification methods and analytical facilities were the same as those described in the preceding paper. Chemical shifts and coupling constants are reported in ppm and in Hz, respectively. The numbering schemes for the NMR data of the PNNP and PNNN ligands are shown in Chart 4.

[(CO)₂Rh(PNNP)Ir(CO)₂]BF₄ (1c). A CH₂Cl₂ solution (3 mL) of **1c** (146 mg, 0.137 mmol) cooled to 0 °C was stirred under a CO atmosphere (1 atm) for 90 min. Precipitation with hexane gave **1c** as a yellowish brown solid, which was washed with ether. **1c** (132 mg, 0.137 mmol, 100% yield): δ_{H} (CDCl₃) 4.00 (4H, d, $J = 10.8$, H6/7), 6.75 (1H, s, H4), 7.5–7.7 (20H, m, Ph); δ_{P} (CDCl₃) 34.8 (s), 41.0 (d, $J_{\text{P-Rh}} = 125$); δ_{C} (CD₂Cl₂) 30.6 (td, $J_{\text{C-H}} = 135$,

$J_{\text{C-P}} = 35$), 30.6 (td, $J_{\text{C-H}} = 135$, $J_{\text{C-P}} = 29$, C6/7), 103.7 (dt, $J_{\text{C-H}} = 189$, $J_{\text{C-P}} = 11$, C4), 126.4–133.3 (d, Ph), 157.8 (br s), 159.4 (br. s, C3/5), the CO peaks could not be located; IR (KBr) 2074, 2007, 1084 cm⁻¹; ESI-MS m/z 843.0 (M⁺ - CO), 815.1 (M⁺ - 2CO), 787.2 (M⁺ - 3CO). Anal. Calcd for C₃₃H₂₅N₂O₄P₂IrRhBF₄: C, 41.39; H, 2.63; N, 2.93. Found: C, 41.75; H, 3.00; N, 2.92.

[(CO)₂Rh(PNNN)Rh(CO)]BF₄ (2a). A CH₂Cl₂ solution (5 mL) of **2a** (158 mg, 0.168 mmol) was stirred for 3 h at room temperature under a CO atmosphere (1 atm). Slow addition of hexane to the resultant mixture gave a yellow precipitate, which was washed with ether and dried in vacuo. **2a** (yellow solid; 141 mg, 0.168 mmol, 100% yield): δ_{H} 3.98 (2H, d, $J = 11.2$, H11), 6.75 (1H, s, H4), 7.28–7.57 (m, aromatic), 7.72 (1H, d, $J = 6.8$, H7), 7.90 (1H, t, $J = 7.8$, H8), 8.40 (1H, br. d, H10); δ_{P} (CDCl₃) 42.6 (d, $J_{\text{P-Rh}} = 126$); δ_{C} (acetone-*d*₆) 103.4 (m, $J_{\text{C-H}} = 174.9$, C4), 122.3 (s, $J_{\text{C-H}} = 169$, C7), 126.0 (d, $J_{\text{C-H}} = 170$, C9), 129.8–133.5 (Ph), 142.8 (d, $J_{\text{C-H}} = 167$, C8), 152.8 (s, C3/5/6), 154.0 (d, $J_{\text{C-H}} = 184$, C10), 156.4 (s), 157.5 (s, C3/5/6), 185.1 (br, CO), 184.4 (br, CO), the C11 signal was overlapped with the solvent signal; IR (KBr) 2101, 2090, 2039, 2019, 1994, 1610, 1084, 1058 cm⁻¹; ESI-MS m/z 631.6 (M⁺ - CO), 575.9 (M⁺ - 3CO). Anal. Calcd for C₂₅H₁₇N₃O₄PRh₂BF₄: C, 40.20; H, 2.29; N, 5.63. Found: C, 39.96; H, 2.59; N, 5.38.

[(CO)₂Ir(PNNN)Ir(CO)₂]BF₄ (2b). **2b** was prepared in a manner similar to the synthesis of **2a**. **2b** (196 mg, 0.21 mmol, 100% yield): δ_{H} (CDCl₃) 4.19 (2H, d, $J = 10.6$, H11), 7.48–8.18 (12H, m, aromatic), 8.18–8.20 (2H, m, H7/8), 8.56 (1H, d, $J = 5.6$, H10); δ_{P} (CDCl₃) 36.7; δ_{C} (CD₂Cl₂) 30.5 (td, $J_{\text{C-H}} = 136$, $J_{\text{C-P}} = 34$, C11), 104.5 (dd, $J_{\text{C-H}} = 183$, $J_{\text{C-P}} = 10$, C4), 122.8 (d, $J_{\text{C-H}} = 172$, C7), 126.2 (d, $J_{\text{C-P}} = 59$, C12), 126.7 (d, $J_{\text{C-H}} = 170$, C9), 129.7–133.2 (Ph), 143.2 (d, $J_{\text{C-H}} = 170$, C8), 152.6 (s, C5/6), 152.7 (d, $J_{\text{C-H}} = 187$, C10), 159.1 (s, C5/6), 159.8 (d, $J_{\text{C-P}} = 4$, C3), 171.4 (s), 172.7 (s), 179.0 (br), 180.0 (br, CO); IR (KBr) 2080, 2008, 1615, 1083 cm⁻¹; ESI-MS m/z 838.0 (M⁺), 810.2 (M⁺ - CO), 782.2 (M⁺ - 2CO), 754.4 (M⁺ - 3CO). Anal. Calcd for C_{27.4}H_{22.6}N₃O₄BF₄PIr₂ (**2b**·0.4(hexane)): C, 34.27; H, 2.37; N, 4.38. Found: C, 34.23; H, 2.49; N, 4.09.

[(CO)₂Rh(PNNN)Ir(CO)₂]BF₄ (2c). A CH₂Cl₂ solution (5 mL) of **2c** (189 mg (0.2 mmol) was stirred for 3 h at 0 °C under a CO atmosphere (1 atm). Addition of hexane gave a brown solid, which was collected and carbonylated for 1 h at room temperature. Precipitation with hexane gave **2c** as an orange solid. **2c** (168 mg, 0.2 mmol, 100% yield): δ_{H} (CD₂Cl₂) 4.05 (2H, d, $J = 11.0$, H11), 7.01 (1H, s, H4), 7.48–7.75 (11H, m, aromatic), 7.97 (1H, d, $J = 7.6$, H7), 8.19 (1H, td, $J = 8.0$, 1.6, H8), 8.63 (1H, d, $J = 5.5$, H10); δ_{P} (CD₂Cl₂) 44.7 (d, $J_{\text{P-Rh}} = 126$); δ_{C} (CD₂Cl₂) 30.4 (td, $J_{\text{C-H}} = 136$, $J_{\text{C-P}} = 29$, C11), 104.3 (dd, $J_{\text{C-H}} = 183$, $J_{\text{C-P}} = 12$, C4), 122.4 (d, $J_{\text{C-H}} = 163$, C7), 126.3 (d, $J_{\text{C-H}} = 165$, C9), 126.6 (d, $J_{\text{C-P}} = 51$, C12), 129.6–132.8 (Ph), 143.1 (d, $J_{\text{C-H}} = 168$, C8), 152.6 (d, $J_{\text{C-H}} = 184$, C10), 153.0 (s), 156.8 (s), 158.5 (s, C3/5/6), 171.9, 173.5 (s, Ir(CO)), 186 (m, Rh(CO)); IR (KBr) 2962, 2073, 1998, 1083 cm⁻¹; ESI-MS m/z 721.9 (M⁺ - CO). Anal. Calcd for C₂₅H₁₇N₃O₄BF₄PIrRh: C, 35.90; H, 2.05; N, 5.02. Found: C, 35.62; H, 2.49; N, 4.64.

[(CO)₂Ir(PNNN)Rh(CO)₂]BF₄ (2d). **2d** was prepared in a manner similar to the synthesis of **1c**. **2d** (yellow solid; 100% yield): δ_{H} (CD₂Cl₂) 4.07 (2H, d, $J = 10.8$, H11), 7.04 (1H, s, H4),

Chart 3

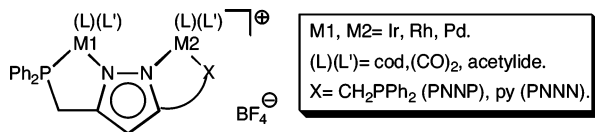
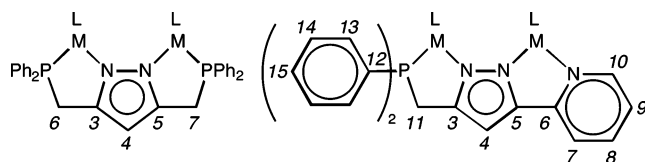


Chart 4



7.49 (1H, t, $J = 6.7$, H9), 7.52–7.80 (10H, m, aromatic), 7.90 (1H, d, $J = 8.0$, H7), 8.12 (1H, t, $J = 7.8$, H8), 8.51 (1H, d, $J = 5.1$, H10); δ_{P} (CD₂Cl₂) 38.8 (s); δ_{C} (CD₂Cl₂) 30.4 (td, $J_{\text{C-H}} = 136$, $J_{\text{C-P}} = 35$, C11), 103.7 (dd, $J_{\text{C-H}} = 181$, $J_{\text{C-P}} = 11$, C4), 122.7 (d, $J_{\text{C-H}} = 168$, C7), 125.9 (d, $J_{\text{C-H}} = 176$, C9), 129.8–133.2 (Ph), 142.4 (d, $J_{\text{C-H}} = 167$, C8), 152.6 (s, C3/5/6), 152.9 (d, $J_{\text{C-H}} = 185$, C10), 158.1 (s), 159.0 (s, C3/5/6), CO signals could not be located; IR (KBr): 2086, 2017, 1972, 1084 cm⁻¹; ESI-MS m/z 721.8 (M⁺ - CO), 693.9 (M⁺ - 2CO). Anal. Calcd for C₂₅H₁₇N₃O₂BF₄PPdIr: C, 35.90; H, 2.05; N, 5.02. Found: C, 35.60; H, 2.51; N, 4.58.

[(CO)₂Ir(PNNP)Pd(allyl)]BF₄ (**3**). **3** was prepared in a manner similar to the synthesis of **2a**. **3** (yellow solid; 100% yield): δ_{H} (CD₂Cl₂) 2.76 (1H, d, $J = 12.0$ Hz, allyl), 3.7–4.2 (6H, m, H6/7 + allyl), 5.45 (1H, m, allyl), 5.7–5.9 (1H, m, allyl), 6.43 (1H, s, H4), 7.4–7.8 (20H, m, Ph); δ_{P} (CDCl₃) 29.5 (s), 35.5 (s); δ_{C} (CD₂Cl₂) 30.7 (td, $J_{\text{C-H}} = 136$, $J_{\text{C-P}} = 35$), 31.0 (td, $J_{\text{C-H}} = 133$, $J_{\text{C-P}} = 27$, C6/7), 52.0 (td, $J_{\text{C-H}} = 154$, $J_{\text{C-P}} = 4$, allyl), 82.7 (td, $J_{\text{C-H}} = 156$, $J_{\text{C-P}} = 29$, allyl), 102.7 (dt, $J_{\text{C-H}} = 178$, $J_{\text{C-P}} = 10$, C4), 119.0 (dd, $J_{\text{C-H}} = 159$, $J_{\text{C-P}} = 6$, allyl), 126.8–133.6 (Ph), 155.8 (d, $J_{\text{C-P}} = 67$), 157.3 (d, $J_{\text{C-P}} = 5$, C3/5), 174.9 (s, CO), 179.8 (br, CO); IR (KBr) 3056, 2925, 2067, 2002, 1959, 1436, 1057 cm⁻¹; ESI-MS m/z 831.3 (M⁺ - CO). Anal. Calcd for C₃₄H₃₀N₂O₂BF₄P₂Ir: C, 43.17; H, 3.20; N, 2.96. Found: C, 43.44; H, 3.36; N, 2.82.

[(CO)₂Ir(PNNN)Pd(allyl)]BF₄ (**4**). **4** was prepared in a manner similar to the synthesis of **1c**. **4** (light brown solid; 100% yield): δ_{H} (CDCl₃) 3.26 (1H, d, $J = 12.8$, allyl), 3.40 (1H, d, $J = 11.9$, allyl), 4.04 (2H, d, $J = 10.9$, H11), 4.17 (1H, d, $J = 6.5$, allyl), 4.57 (1H, d, $J = 6.2$, allyl), 5.77 (1H, m, allyl), 7.11 (1H, s, H4), 7.35 (1H, t, $J = 7.0$, H9), 7.45–8.00 (12H, m, aromatic), 8.53 (1H, d, $J = 5.3$, H10); δ_{P} (CD₂Cl₂) 39.0; δ_{C} (CD₂Cl₂) 30.4 (td, $J_{\text{C-H}} = 135$, $J_{\text{C-P}} = 33$, C11), 62.2 (t, $J_{\text{C-H}} = 162$, allyl), 62.9 (t, $J_{\text{C-H}} = 161$, allyl), 102.1 (dd, $J_{\text{C-H}} = 179$, $J_{\text{C-P}} = 8$, C4), 116.8 (d, $J_{\text{C-H}} = 163$, allyl), 121.8 (d, $J_{\text{C-H}} = 169$, C7), 124.9 (d, $J_{\text{C-H}} = 169$, C9), 129.6–133.0 (Ph), 140.4 (d, $J_{\text{C-H}} = 167$, C8), 151.7 (s, C3/5/6), 153.8 (d, $J_{\text{C-H}} = 183$, C10), 156.4 (s), 157.0 (s, C3/5/6), 179.5 (s), 180.0 (d, $J_{\text{C-P}} = 84$, CO); IR (KBr) 2070, 2005, 1607, 1451, 1082 cm⁻¹; ESI-MS m/z 710.2 (M⁺ - CO), 738.1 (M⁺), 750.8 (M⁺ - CO + MeCN), eluted with MeCN. Anal. Calcd for C₂₆H₂₂N₃O₂BF₄PPdIr: C, 37.86; H, 2.69; N, 5.09. Found: C, 38.32; H, 2.91; N, 4.83.

[(allyl)Pd(PNNN)Ir(CO)₂]BF₄ (**5**). **5** was prepared in a manner similar to the synthesis of **2a**. **5** (dark violet solid; 98% yield): δ_{H} (CD₂Cl₂) 2.77 (1H, d, $J = 12$, allyl), 3.90–4.13 (4H, m, allyl + H11), 5.42 (1H, t, $J = 1.4$, allyl), 5.74 (1H, m, allyl), 6.91 (1H, s, H4), 7.44–7.64 (11H, m, aromatic), 7.90 (1H, d, $J = 8.4$, H7), 8.14 (1H, td, $J = 7.6$, 1.2, H8), 8.61 (1H, d, $J = 5.2$, H10); δ_{P} (CD₂Cl₂) 32.1 (s); δ_{C} (CD₂Cl₂) 30.6 (td, $J_{\text{C-H}} = 134$, $J_{\text{C-P}} = 26$, C11), 51.9 (td, $J_{\text{C-H}} = 160$, $J_{\text{C-P}} = 4$, allyl), 83.0 (td, $J_{\text{C-H}} = 154$, $J_{\text{C-P}} = 29$, allyl), 103.9 (dd, $J_{\text{C-H}} = 181$, $J_{\text{C-P}} = 9$, C4), 119.4 (dd, $J_{\text{C-H}} = 161$, $J_{\text{C-P}} = 6$, allyl), 121.9 (d, $J_{\text{C-H}} = 167$, C7), 125.7 (d, $J_{\text{C-H}} = 170$, C9), 129.5–133.2 (Ph), 142.9 (d, $J_{\text{C-H}} = 166$, C8), 152.6 (d, $J_{\text{C-H}} = 183$, C10), 154.1 (s, C5/6), 155.4 (d, $J_{\text{C-P}} = 8$, C3), 157.3 (s, C5/6), 172.3 (s), 175.0 (s, CO); IR (KBr) 2067, 2001, 1616, 1461, 1056 cm⁻¹; ESI-MS m/z 738.1 (M⁺), 698.1 (M⁺ - allyl), 669.2 (M⁺ - allyl - CO). Anal. Calcd for C₂₆H₂₂N₃O₂BF₄PPdIr: C, 37.86; H, 2.68; N, 5.09. Found: C, 37.65; H, 2.86; N, 4.95.

[(CO)₂Rh(O=PNNN)Rh(CO)₂]BF₄ (**7**). A CD₂Cl₂ solution of **1a** was stirred under an O₂ atmosphere (1 atm) for 1 day, and a complete conversion to **7** was confirmed by ¹H and ³¹P NMR. **7**: δ_{H} (CD₂Cl₂) 4.23 (2H, d, H11), 6.97 (1H, s, H4), 7.3–7.8 (12 H, aromatic), 8.06 (1H, t, $J = 7.8$, H8), 8.47 (1H, d, $J = 5.2$, H10); δ_{P} (CD₂Cl₂) 37.2 (s); IR (KBr) 2084, 2016, 1083 cm⁻¹; ESI-MS m/z 675.8 (M⁺), 647.5 (M⁺ - CO), 619.8 (M⁺ - 2CO), 564.2

(M⁺ - 4CO). Anal. Calcd for C₂₆H₂₂N₃O₂BF₄PPdIr: C, 37.86; H, 2.68; N, 5.09. Found: C, 37.65; H, 2.86; N, 4.95.

(CO)Ir(PNNP)Ir(CO)(μ -C≡C-*p*-tol) (**10ba**). To a THF solution (10 mL) of 2 equiv of HC≡C-*p*-tol (36 μ L, 0.287 mmol) cooled to -75 °C was added *n*-BuLi (1.6 M, 188 μ L, 0.300 mmol). After 10 min, **1c** (150 mg, 0.140 mmol) dissolved in THF (10 mL) was added to the resultant solution. The mixture was stirred for 10 min at -75 °C, for 30 min at 0 °C, and for 1 h at ambient temperature. The solution was filtered through an alumina pad and concentrated to 2 mL under reduced pressure. Addition of diethyl ether gave **10ba** as a yellow precipitate. **10ba** (48 mg, 0.046 mmol, 33% yield): δ_{H} (CD₂Cl₂) 2.29 (3H, s, Me), 3.88 (4H, d, $J = 10.9$, H6/7), 6.05 (1H, s, H4), 7.10 (4H, d, $J = 12.0$, tol), 7.30–7.74 (22H, m, aromatic); δ_{P} (CD₂Cl₂) 37.0 (s); δ_{C} (CD₂Cl₂) 21.2 (q, $J_{\text{C-H}} = 126$, Me), 35.4 (td, $J_{\text{C-H}} = 134$, $J_{\text{C-P}} = 33$, C6/7), 99.2 (dt, $J_{\text{C-H}} = 176$, $J_{\text{P-C}} = 10$, C4), 107.3 (t, $J = 20$, C9), 121.6 (t, $J = 57$, C8), 125.5–137.9 (Ph), 153.1 (d, $J_{\text{C-P}} = 6$, C3/5), 182.0 (d, $J_{\text{C-P}} = 9$, CO); IR (KBr) 3054, 2918, 2025, 1964, 1505, 1101 cm⁻¹; FD-MS m/z 1020 (M⁺). Anal. Calcd for C₄₀H₃₂N₂O₂P₂Ir₂: C, 47.14; H, 3.17; N, 2.75. Found: C, 46.40; H, 3.31; N, 2.74.

(CO)Ir(PNNP)Ir(CO)(μ -C≡CSiMe₃) (**10bb**). **10bb** was prepared in a manner similar to the synthesis of **10ba**. **10bb** (yellow solid; 53% yield): δ_{H} (CD₂Cl₂) 0.41 (9H, s, SiMe₃), 3.95 (4H, d, $J = 10.6$, H6/7), 6.12 (1H, s, H4), 7.45–7.76 (20H, m, Ph); δ_{P} (CD₂Cl₂) 34.8 (s); δ_{C} (CD₂Cl₂) 1.4 (s, $J_{\text{C-H}} = 120$, SiMe₃), 36.3 (td, $J_{\text{C-H}} = 134$, $J_{\text{C-P}} = 33$, C6/7), 99.0 (dd, $J_{\text{C-H}} = 176$, $J = 9$, C4), 104.7 (s, 9, C β), 128.7–132.9 (Ph), 155.7 (dt, $J = 13$, 9, C3/5); IR (KBr) 2034, 1973, 1890 cm⁻¹; FD-MS m/z 1001 (M⁺). Anal. Calcd for C₃₆H₃₄N₂O₂SiP₂Ir₂: C, 43.19; H, 3.42; N, 2.80. Found: C, 43.46; H, 3.47; N, 2.80.

(CO)Rh(PNNP)Ir(CO)(μ -C≡C-Tol) (**10ca**). **10ca** was prepared in a manner similar to the synthesis of **10ba**. **10ca** (yellow brown solid; 65% yield): δ_{H} (C₆D₆) 1.93 (3H, s, Me), 3.39 (4H, dd, $J = 10.2$, 2.9, H6/7), 5.68 (1H, s, H4), 7.3–7.7 (22H, m, aromatic), 7.9 (2H, d, $J = 8.2$, tol); δ_{P} (C₆D₆) 35.3 (s), 51.6 (d, $J_{\text{P-Rh}} = 158$); δ_{C} (C₆D₆) 21.4 (q, $J_{\text{C-H}} = 125$, Me), 35.0 (td, $J_{\text{C-H}} = 133$, $J_{\text{C-P}} = 28$, C7), 35.9 (td, $J_{\text{C-H}} = 130$, $J_{\text{C-P}} = 31$, C7), 99.1 (br d, $J_{\text{C-H}} = 170$, C4), 105.6 (br, C≡C β), 120.0 (d, $J_{\text{C-P}} = 114$, C α ≡C), 128.7–133.6 (aromatic), 151.7 (d, $J_{\text{C-P}} = 7$), 155.9 ($J_{\text{C-P}} = 12$, C6/7), 184.5 (s), 195 (m, CO); IR (KBr) 3052, 2961, 1978, 1946, 1434, 1101 cm⁻¹; FD-MS m/z 930 (M⁺). Anal. Calcd for C_{40.5}H₃₃N₂O₂P₂ClRhIr (**10ca**·0.5CH₂Cl₂): C, 50.03; H, 3.42; N, 2.88. Found: C, 49.84; H, 3.38; N, 2.88.

(CO)Rh(PNNP)Ir(CO)(μ -C≡CSiMe₃) (**10cb**). **10cb** was prepared in a manner similar to the synthesis of **10ba**. **10cb** (yellow-brown solid; 88% yield): δ_{H} (acetone-*d*₆) 0.34 (9H, s, SiMe₃), 3.90 (2H, d, $J = 10.4$), 4.04 (2H, d, $J = 11.1$, H6/7), 6.01 (1H, s, H4), 7.4–7.8 (20H, m, Ph); δ_{P} (acetone-*d*₆) 39.8 (s), 56.1 (d, $J_{\text{P-Rh}} = 160$); δ_{C} (C₆D₆) 2.7 (s, SiMe₃), 35.9 (d, $J_{\text{C-P}} = 27$), 36.3 (d, $J_{\text{C-P}} = 29$, C6/7), 99.1 (br, C4), 128.7–135.2 (Ph), 152.4 (d, $J_{\text{C-P}} = 9$), 156.3 ($J_{\text{C-P}} = 8$, C3/5), 184.3 (br), 187.7 (br, CO); IR (KBr) 1971, 1940, 1901, 1434, 1100 cm⁻¹; FD-MS m/z 912 (M⁺).¹⁵

(CO)Rh(PNNN)Rh(CO)(μ -C≡C-*p*-tol) (**11aa**). **11aa** was prepared in a manner similar to the synthesis of **10ba**, and workup should be done at 0 °C because of its thermal instability. **11aa** (yellow-brown solid; 63% yield): δ_{H} (acetone-*d*₆) 2.31 (3H, s, Me), 4.09 (2H, d, $J = 11.3$, H11), 6.67 (1H, s, H4), 7.12 (2H, d, tol), 7.34 (1H, t, $J = 3.6$, H9), 7.53–7.62 (7H, m, aromatic), 8.00 (1H, t, $J = 7.8$, H8), 7.73–7.89 (6H, m, aromatic), 8.66 (1H, d, $J = 5.3$, H10); δ_{P} (acetone-*d*₆) 58.5 (d, $J_{\text{P-Rh}} = 158$); δ_{C} (CD₂Cl₂ at 0 °C) 21.1 (s, Me), 34.0 (d, $J_{\text{C-P}} = 28$, C11), 99.2 (d, $J_{\text{C-P}} = 12$, C4), 120.2 (s, C7), 123.4 (s, C9), 126.7–136.5 (aromatic), 137.8 (s, C8), 151.8 (s, C3/5/6), 153.0 (s, C10), 153.9 (s, C3/5/6), 192.4 (dd, $J_{\text{C-Rh}} = 66$, $J_{\text{C-P}} = 13$), 193.8 (d, $J_{\text{C-Rh}} = 7$, CO); IR (KBr)

(15) Because of the instability of the complexes satisfactory ¹³C NMR data and elemental analyses have not been obtained.

Table 2. Crystallographic Data

	2a/7 ^a	10ca	11ab	5	6
solvent	CH ₂ Cl ₂	3C ₆ H ₆		CH ₂ Cl ₂	4CHCl ₃
formula	C ₅₁ H ₃₆ N ₆ O ₉ B ₂ F ₈ P ₂ Cl ₂ Rh ₄	C ₅₈ H ₅₀ N ₂ O ₂ P ₂ RhIr	C ₂₈ H ₂₆ N ₃ O ₂ SiPRh ₂	C ₂₇ H ₂₄ N ₃ O ₂ BF ₄ PCl ₂ PdIr	C ₅₂ H ₄₈ N ₂ O ₄ B ₂ F ₈ P ₂ Cl ₁₂ Ir ₂
formula wt	1594.96	1164.12	701.40	909.81	1810.39
cryst syst	triclinic	triclinic	monoclinic	monoclinic	triclinic
space group	<i>P</i> $\bar{1}$	<i>P</i> $\bar{1}$	<i>P</i> ₂ / <i>c</i>	<i>P</i> ₂ / <i>c</i>	<i>P</i> $\bar{1}$
<i>a</i> /Å	9.990(4)	12.835(9)	13.491(8)	9.239(7)	13.235(7)
<i>b</i> /Å	13.054(3)	14.471(8)	11.856(3)	9.09(1)	14.245(9)
<i>c</i> /Å	22.616(8)	15.382(8)	17.317(10)	36.77(2)	19.86(1)
α /deg	90.35(2)	63.10(2)	90	90	105.27(2)
β /deg	99.879(7)	89.46(3)	102.72(1)	96.01(9)	106.60(2)
γ /deg	96.11(2)	86.39(3)	90	90	98.09(2)
<i>V</i> /Å ³	2888(1)	2542(2)	2701(2)	3069(4)	3366(3)
<i>Z</i>	2	2	4	4	2
<i>d</i> _{calcd} /g cm ⁻³	1.834	1.521	1.724	1.968	1.786
μ /mm ⁻¹	1.353	3.052	1.353	5.209	4.548
no. of diffractions collected	19 839	6484	16 544	7930	21 506
no. of variables	757	521	334	368	757
R1 for data with <i>I</i> > 2 σ (<i>I</i>)	0.0866 (for 6774 data)	0.0703 (for 2757 data)	0.0711 (for 1961 data)	0.0438 (for 4568 data)	0.0622 (for 8941 data)
wR2	0.2329 (for all 11 387 data)	0.1817 (for all 5302 data)	0.2125 (for all 5925 data)	0.1599 (for all 7028 data)	0.1691 (for all 13 065 data)

^a 2a and 7 formed cocrystals.

1980 cm⁻¹; Anal. Calcd for C₃₃H₂₆N₃O₂PCl₂Rh₂ (11aa·CH₂Cl₂): C, 49.28; H, 3.26; N, 5.22. Found: C, 49.23; H, 3.39; N, 5.07.

(CO)Rh(PNNN)Rh(CO)(μ -C≡CSiMe₃) (11ab). 11ab was prepared in a manner similar to the synthesis of 11aa. 11ab (yellow-brown solid; 46% yield): δ_{H} (acetone-*d*₆) 0.33 (9H, s, SiMe₃), 4.04 (2H, d, *J* = 11.3, H11), 6.65 (1H, s, H4), 7.52–7.88 (12H, m, aromatic), 8.00 (1H, t, *J* = 7.8, H8), 8.56 (1H, d, *J* = 5.3, H10); δ_{P} (acetone-*d*₆) 58.2 (d, *J*_{P-Rh} = 163); δ_{C} {¹H} (CD₂Cl₂) 1.8 (s, C16), 34.2 (d, *J*_{C-P} = 28, C11) 98.9 (d, *J*_{C-P} = 11, C4), 120.1 (s, C7), 123.4 (s, C9), 128.7–132.9 (Ph), 138.0 (s, C8), 152.2 (s, C3/5/6), 152.8 (s, C10), 153.8 (s, C3/5/6), 193 (br, CO); IR (KBr) 1975, 1891, 1607 cm⁻¹.¹⁵

(CO)Rh(PNNN)Ir(CO)(μ -C≡C-*p*-tol) (11ca). 11ca was prepared in a manner similar to the synthesis of 10ba. 11ca (yellow solid; 35% yield): δ_{H} (C₆D₆) 1.98 (3H, s, Me), 3.38 (2H, d, *J* = 9.4, H11), 5.82 (1H, s, H4), 5.98 (1H, t, *J* = 6.1, H9), 6.7–7.8 (aromatic), 8.16 (2H, d, *J* = 7.8, tol); δ_{P} (C₆D₆) 53.0 (d, *J*_{P-Rh} = 161); δ_{C} decomposed during data collection.¹⁵

[(μ -C≡C-*p*-tol){(CO)Rh(PNNP)Ir(CO)}₂]BF₄ (12b). To a CH₂Cl₂ solution (5 mL) of 10cb (43.4 mg, 0.0475 mmol) cooled to 0 °C was added 1c (45 mg, 0.0475 mmol) slowly as a solid. After the solution was stirred for 1 h at 0 °C, ether was slowly added to give a red solid, which was collected, washed with ether, and dried in vacuo. 12b (81 mg, 0.0442 mmol, 93% yield): δ_{H} (acetone-*d*₆) 2.24 (s, 3H, Me), 3.9–4.4 (m, 8H, H6 + H7), 6.36 (s, 2H, H4), 6.78 (d, *J* = 8.2, 2H, tol), 7.4–7.9 (m, 42H, aromatic); δ_{P} (acetone-*d*₆) 44.7 (s), 58.5 (d, *J*_{Rh-P} = 197); δ_{C} (acetone-*d*₆) 21.2 (s, Me), 32.2 (d, *J*_{C-P} = 36), 33.0 (d, *J*_{C-P} = 29, C6/7), 100.7 (t, *J*_{C-P} = 12, C4), 117.3 (d, *J*_{C-P} = 96, C_a), 128.6–135.6 (aromatic), 154.0 (s), 156.0 (C3/5), 176.7 (bs, CO), 191.6 (dd, *J*_{Rh-C}, *p*-C = 67, 13, CO); IR (KBr) 1976, 1633, 1084 cm⁻¹; ESI-MS: *m/z* 1744.9 (M⁺).¹⁵

Hydrogenation of Diphenylacetylene. A glass autoclave was charged with diphenylacetylene (1 mmol), catalyst (0.01 mmol), cumene (10 μ L), and THF (2 mL). After two freeze–pump–thaw cycles H₂ was pressurized to 5 atm. Products were identified and quantified by GC-MS analysis.

Hydroformylation of 1-Octene. A stainless autoclave was charged with 1-octene (1 mmol), cocatalyst (0.02 mmol), cumene (10 μ L), and THF (2 mL). After two freeze–pump–thaw cycles H₂ (15 atm) and CO (15 atm) was pressurized. The autoclave was heated for 6 h at 80 °C. Products were identified and quantified by GC-MS analysis.

Allylation of Aniline Giving Mono- and Diallylaniline. A 50 mL Schlenk tube was charged with aniline (1 mmol), allyl alcohol (4 mmol), MgSO₄ (250 mg), cumene (10 μ L), catalyst (0.02 mmol), and THF (2 mL). After two freeze–pump–thaw cycles the mixture was heated under CO (1 atm) for 6 h at 80 °C. Products were identified and quantified by GC-MS analysis.

X-ray Crystallography. Single crystals of 2a·CH₂Cl₂, 5·CH₂Cl₂, and 11ab were obtained by recrystallization from CH₂Cl₂. 6 from CHCl₃, and 10ca·3C₆H₆ from C₆H₆. The experimental procedures were the same as those described in the preceding paper. Diffraction measurements, except for 5, were made on a Rigaku RAXIS IV imaging plate area detector with Mo K α radiation (λ = 0.710 69 Å) at –60 °C. For the data collection of 5, diffraction measurements were made on a Rigaku AFC7R automated four-circle diffractometer by using graphite-monochromated Mo K α radiation (λ = 0.710 69 Å) at room temperature. Crystallographic data for 2a/7, 10ca, 11ab, 5, and 6 are given in Table 2.

Unless otherwise stated, all non-hydrogen atoms were refined anisotropically, methyl hydrogen atoms were refined using riding models, and other hydrogen atoms were fixed at the calculated positions. For 5, the CH₂Cl₂ solvate molecule was refined with isotropic thermal parameters and two components for the central carbon atom were considered (C51:C52 = 0.5:0.5). Hydrogen atoms attached to the CH₂Cl₂ molecule were not included in the refinement. For 10ca, the disordered phenyl group (C51–C56) was refined with isotropic thermal parameters by taking into account two components (C52–C53–C55–C56:C52A–C53A–C55A–C56A = 0.523:0.477). Two of the three benzene solvate molecules were refined isotropically. Hydrogen atoms attached to the disordered part and the solvate molecules were not included in the refinement.

Acknowledgment. We are grateful to the Ministry of Education, Culture, Sports, Science and Technology of the Japanese Government and the Japan Society for Promotion of Science and Technology for financial support of this research. A Monbukagakusho scholarship for C.D. from the Japanese Government is gratefully acknowledged.

Supporting Information Available: Tables and figures giving crystallographic results (11 pages); data are also available as CIF files. This material is available free of charge via the Internet at <http://pubs.acs.org>.

OM050897E